
Article:
Zhang, K., Li, G.-J. orcid.org/0000-0002-5956-4033, Zhu, Z. et al. (1 more author) (2021) Impact of current harmonic injection on performance of multi-phase synchronous reluctance machines. IEEE Transactions on Energy Conversion, 36 (3). pp. 1649-1659. ISSN 0885-8969

https://doi.org/10.1109/TEC.2020.3041252

Impact of Current Harmonic Injection on Performance of Multi-Phase Synchronous Reluctance Machines

K. Zhang, G. J. Li, *Senior Member*, *IEEE*, Z. Q. Zhu, *Fellow*, *IEEE*, and G. W. Jewell

***Abstract*—This paper combines the use of multi-phase configurations and current harmonic injection methods to achieve significantly improved performance for doubly salient synchronous reluctance machines (DS-SRMs). In order to understand the torque production mechanism of multi-phase DS-SRMs with current harmonic injection, some general analytical torque models have been developed. The models are based on Fourier Series analysis of self- and mutual-inductances. It has been established that with current harmonic injection, the torque ripple of both 5-phase and 6-phase DS-SRMs can be significantly reduced and the average torque can be enhanced. It contrast, harmonic injection always has a detrimental impact on 4-phase machines. The investigations of losses and dynamic performance with current harmonic injection for multi-phase machine have also been carried out and demonstrated that the proposed method can improve the efficiency in constant torque region and maintain comparable performance to fundamental current supply in the flux weakening region. Experimental validation based on single layer, 6-phase, DS-SRM has been performed.**

***Index Terms*—Current harmonic injection, doubly-salient, multiphase, synchronous reluctance machine.**

I. Introduction

DOUBLY salient synchronous reluctance machines (DS-SRMs) have received increasing attention in the recent years due to the features such as simple and robust rotor structure, straightforward manufacture and good fault-tolerance. Furthermore, the absence of rotor permanent magnets yields a significant potential cost saving and makes them well-suited to deployment in sectors such as electric vehicles, aerospace and other safety-critical applications [1]. Doubly salient synchronous reluctance machines (DS-SRMs) have, to a large extent, evolved from switched reluctance machines by supplying them with sinewave current instead of square wave currents encountered in switched reluctance machines (conduction angle of 120 electrical degrees) [2]. In this sinusoidal mode of operation, the rotor rotates at the same speed as the stator armature field, leading to the synchronous nature of the machine. It is now well-established that vibrations and acoustic noise can be markedly reduced by supplying a given machine with sinewave current instead of the normal switched reluctance square-wave operation [3]-[4]. However, a straightforward substitution of sine-wave current waveform for a square-wave waveform halves the average torque capability for the same rms current. In order to enhance the average torque to a competitive level while retain the ability to supply the DS-SRMs with sinewave currents, new winding configurations, viz. double-layer and single-layer mutually coupled windings have been proposed according to classical winding theory for synchronous reluctance machines. It has been shown in [5]-[6] that the new winding configuration can achieve much improved torque capability, especially for the double layer machines, e.g. 77% additional average torque at high phase current compared to their conventional counterpart. However, due to the nature of both the self- and mutual-inductances, the mutually coupled machines generate much higher torque ripple. To mitigate this issue, several studies have focused on design aspects, e.g., stator/rotor skewing and shaping [7]-[8] to yield an air gap flux density which is more sinusoidal. Other studies have concentrated on control aspects, for example through direct instantaneous torque control (DITC) [9] and phase current shaping (or optimization) [10]-[11]. With several commonalities with current shaping, a new current harmonic injection method has been proposed for 3-phase DS-SRMs in [12]-[13]. Such a method can quantify the torque contribution due to each inductance harmonic, both with and without current harmonic injection. As a result, it allows an appropriate selection of current harmonics (in terms of order, magnitude, phase angle) to improve the overall torque performance of 3-phase DS-SRMs.

Since current shaping or harmonic current injection will introduce higher order harmonic currents, it is likely to increase core losses in the machines, and hence lead to reduced efficiency. Therefore, if maintaining sinewave current is deemed desirable, increasing the phase number (m) may be another effective means of reducing torque ripple [14]-[15]. In addition, machines with higher phase number (m>3) can also achieve higher torque density and enhanced fault-tolerant capability [16]-[17].

Research has been reported on combining multi-phase machines with harmonic current injection to further reduce torque ripple [19]. However, these methods were developed for permanent magnet machines and no corresponding research has been carried out for multi-phase DS-SRMs. The latter have vastly different characteristics compared to permanent magnet machines due to their doubly salient structure, with torque being generated solely by the variations of self- and mutual-inductances. Previous studies have demonstrated that the multi-phase DS-SRM also have different characteristics compared to their 3-phase counterparts with sinewave current supply, e.g. more different types of mutual-inductances [15]. Hence, if harmonic current is injected into a multi-phase DS-SRMs, it is likely that it will behave differently compared to its 3-phase counterpart. This is particularly the case for dynamic aspects of performance such as torque-speed curves, power-speed curves, power-factor speed curves, and efficiency maps, etc. This paper investigates the impact of harmonic current injection on multi-

phase DS-SRMs. Underpinning this investigation is the development of a generalised analytical torque model based on Fourier Series analysis of the self- and mutual-inductances. This facilitates the selection of the features of injected current harmonics, such as the order, magnitude and phase angle required to achieve a particular performance objective such as maximum average torque or minimum torque ripple. A range of phase numbers (up to 6-phases) with different slot/pole number combinations and winding configurations, viz. double-layer (DL) and single-layer (SL), will be investigated in this paper.

The main contribution of this paper is to establish several general guidelines for performance (both static and dynamic) improvement of multi-phase DS-SRMs using current harmonic injection.

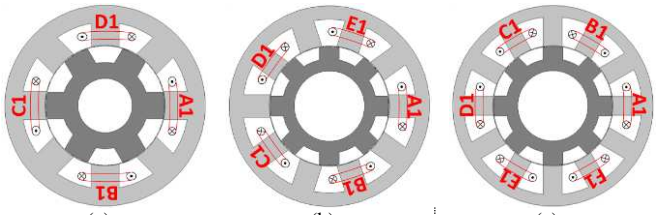

(a) (b) (c)

Fig. 1. Common DS-SRMs topologies. (a) 8s/6p 4-phase, (b) 10s/8p 5-phase, (c) 12s/8p 6-phase. Here, only SL windings are given, the DL windings will have the same number of turns per phase but with double number of coils.

TABLE I MACHINE KEY SPECIFICATIONS (THE RATED VALUES ARE FOR THE SL 6-PHASE VARIANT)

Stator outer radius (mm)	45	Slot fill factor	0.37
Split ratio	0.6	Rated RMS current (A)	5
Air gap length (mm)	0.5	Rated speed (rpm)	400
Active length (mm)	60	Rated torque (Nm)	2.4
N° of turns/phase	132	Rated power (W)	100

II. TORQUE MODEL WITH CURRENT HARMONIC INJECTION

The proposed current harmonic injection methodology can be divided into two distinct steps. In the first step, the derivation of expressions for the instantaneous torque using inductances obtained by 2D-FEA is carried out. In the second step, the expressions for the instantaneous torque are deployed to establish the relationship between torque waveform and the injected current harmonic, which in turn facilities the selection of the current harmonic features (order, magnitude and phase angle) to which increase average torque and/or lower torque ripple as well as impacting favorably on dynamic performance.

Fig. 1 shows typical DS-SRMs with different slot/pole number combinations and different winding configurations. The key parameters for all these variants are given in TABLE I where the rated values are only for the SL 6-phase machine. Setting aside for the time being, consideration of magnetic saturation, the instantaneous torque equation of multi-phase DS-SRMs can be expressed as (1) [5]-[6].

$$T_e = \frac{1}{2}[i_m]^T \frac{d[L_m]}{d\theta}[i_m] \quad (1)$$

where $[i_m] = [i_1, i_2, \cdots i_m]^T$ is the phase current matrix, $[L_m]$ represents $m \times m$ inductance matrix. θ is the mechanical rotor position and m is the phase number. In order to investigate the contribution of particular order current harmonics to the torque profile, a stator current with single current harmonic injection can be expressed by (2). It is worth noting that only phase 'a' is given here because other phases will have the same magnitude while with a $2\pi/m$ phase shift.

$$I_a = I_f \sin(\theta_e + \beta_f) + I_v \sin(v\theta_e + \beta_v) \quad (2)$$

where I_f and β_f are the amplitude and phase angle of the fundamental current, whilst I_v and β_v represent the amplitude and phase angle of the v^{th} order current harmonic, respectively. θ_e is the electrical rotor position. Based on the study in [15], there will be one type of self-inductance waveform and Z types of mutual-inductance waveform for an m-phase DS-SRM. The factor Z depends on the phase number and is be the minimum integer which is no less than $(m-1)/2$. By way of example, for the 12slot/8pole single layer 6-phase machine shown in Fig. 1(b), 3 different mutual-inductance waveforms will be generated since $(m-1)/2 = 2.5 < 3$. The self- and mutual-flux linkage at different rotor positions when phase 'a' is supplied with different dc currents are shown in Fig. 2, where Φ_a is the self-flux linkage of phase 'a' and Φ_{ab} is the mutual-flux linkage between phases 'a' and 'b', etc. In this case the onset of appreciable magnetic saturation occurs in this 6-phase DS-SRM at a current of ~8A. Under linear magnetic conditions (i.e. current level below 8A or so), the self- and mutual-inductance can be calculated. The resulting variation in the various self- and mutual-inductance components with rotor position are shown in Fig. 3.

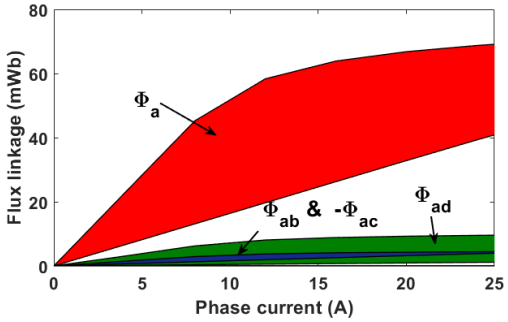

Fig. 2. Self- and mutual-flux linkages of the SL 6-phase DS-SRM, when phase 'a' is supplied with dc current. In this figure, $\Phi_{ab} = -\Phi_{ac}$.

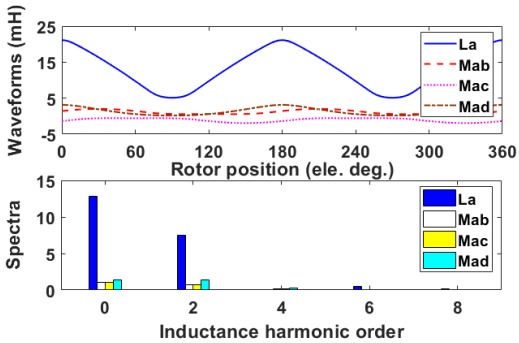

Fig. 3. Inductance waveforms and spectra for a SL 6-phase DS-SRM, when phase 'a' is supplied with 1A dc current.

The self- and mutual-inductances variations with rotor angular position can be expressed as Fourier Series:

$$L = L_0 + \sum_{n=1}^{\infty} L_n \cos(n\theta_e + \alpha_n) \quad (3)$$

$$M_x = M_{x0} + \sum_{n=1}^{\infty} M_{xn} \cos(n\theta_e + \alpha'_{xn}) \quad (4)$$

where L and M_x are the self- and mutual-inductances, respectively. α_n and α'_n are the phase angle of the n^{th} order self- and mutual-inductance harmonics. The subscript '0' denotes the dc component while the subscript 'x' is utilized to represent the different components of mutual-inductance and $x \in (1, 2, \ldots, Z)$. When 'x' is equal to '1', M_1 represents a mutual-inductance between two adjacent phases, such as, M_{ab}, M_{ac} and so on, while M_2 represents a mutual-inductance between two phases with an interval of one phase, such as, M_{ac}, M_{bd} and so on.

Substituting (2), (3) and (4) into (1) allows the instantaneous torque equation to be transformed as below:

$$T_e = T_f + T_h \tag{5}$$

With

$$\begin{cases} T_f = T_{fsel} + T_{fmut} = T_{f0} + T_{frip} \\ T_h = T_{hsel} + T_{hmut} = T_{h0} + T_{hrip} \end{cases} \tag{6}$$

where the subscripts 'f' and 'h' represent the components due to fundamental and harmonic currents; '*sel*' and '*mut*' are the torques produced by self- and mutual-inductances; '0' and '*rip*' are the average torque and torque ripple, respectively.

The torque produced by sinewave current for m-phase machines has been investigated in [15]. This section will further detail the torque components produced by the interaction between current harmonics and self-/mutual-inductances, which can be decoupled into two terms: $T_h(I_f I_v)$ and $T_h(I_v^2)$. This paper will focus on the harmonic torque term $T_h(I_f I_v)$ as this tends to be the dominant term in terms of improving torque performance. However, to enhance the accuracy of the prediction of instantaneous torque, the calculation of $T_h(I_v^2)$ may also need to be investigated, which has not been detailed in this paper due to space limitations. The constituent components of $T_h(I_f I_v)$ are given by:

$$\begin{aligned} T_{hsel} = \frac{mp}{2}\sum_{n=1}^{\infty}\frac{nL_n}{2} I_f I_v \{ & \sin(A\theta_e + \beta_1 + \beta_v + \alpha_n) \\ & - \sin(B\theta_e + \beta_1 + \beta_v - \alpha_n) \\ & - \sin(C\theta_e + \beta_1 - \beta_v + \alpha_n) \\ & + \sin(D\theta_e + \beta_1 - \beta_v - \alpha_n)\} \end{aligned} \tag{7}$$

And

$$\begin{aligned} T_{hmut} = \frac{mp}{2}\sum_{n=1}^{\infty}\sum_{x=1}^{Z} c\frac{nM_{xn}}{2} I_f I_v \\ \Big\{ & \sin\Big(A\theta_e + \beta_1 + \beta_v + \alpha'_{xn} - \frac{2\pi}{m}vx\Big) \\ & - \sin\Big(B\theta_e + \beta_1 + \beta_v - \alpha'_{xn} - \frac{2\pi}{m}vx\Big) \\ & - \sin\Big(C\theta_e + \beta_1 - \beta_v + \alpha'_{xn} + \frac{2\pi}{m}vx\Big) \\ & + \sin\Big(D\theta_e + \beta_1 - \beta_v - \alpha'_{xn} + \frac{2\pi}{m}vx\Big) \\ & + \sin\Big(A\theta_e + \beta_1 + \beta_v + \alpha'_{xn} - \frac{2\pi}{m}x\Big) \\ & - \sin\Big(B\theta_e + \beta_1 + \beta_v - \alpha'_{xn} - \frac{2\pi}{m}x\Big) \\ & - \sin\Big(C\theta_e + \beta_1 - \beta_v + \alpha'_{xn} - \frac{2\pi}{m}x\Big) \\ & + \sin\Big(D\theta_e + \beta_1 - \beta_v - \alpha'_{xn} - \frac{2\pi}{m}x\Big)\Big\} \end{aligned} \tag{8}$$

And

$$\begin{cases} A = 1 + v + n \\ B = 1 + v - n \\ C = 1 - v + n \\ D = 1 - v - n \end{cases} \tag{9}$$

$$c = \begin{cases} 0.5 & mod(m,2) = 0 \text{ and } x = Z \\ 1 & otherwise \end{cases}$$

$A, B, C, D = mk$ where k is 0, 1, 2, 3…

According to (7)-(9), it can be seen that the frequency of T_h is related to the order of injected current harmonic v and inductance harmonic n, which is described by

$$|1 \pm v \pm n| = mk \tag{10}$$

As can be proved that the T_h only contains the mk^{th} order torque harmonic, which is the same as that of T_f (as detailed in [15]). Therefore, it is possible to compensate for torque ripple produced by the fundamental current using a contribution produced by a current harmonic. When the injected current harmonic order is selected, the active inductance harmonic order related to the desired torque harmonic can be determined at the same time as:

$$n = |mk \pm v \pm 1| \tag{11}$$

Moreover, it can be proven that an average torque due to the injected current harmonic can be produced when the factor of θ_e (A, B, C or D) is equal to 0. It therefore follows that when the v^{th} order current harmonic is injected, the $(v \pm 1)^{th}$ order inductance will contribute to average torque, as described by (12).

$$\begin{aligned} T_{h0} = -\frac{mp(v \mp 1)}{4} I_f I_v \{ & L_{v\mp1} \sin(\beta_1 \mp \beta_v \pm \alpha_{v\mp1}) \\ & + \sum_{x=1}^{Z} cM_{x(v\mp1)} \Big[\sin\Big(\beta_1 \mp \beta_v \pm \alpha'_{x(v\mp1)} \pm \frac{2\pi}{m}xv\Big) \\ & + \sin\Big(\beta_1 \mp \beta_v \pm \alpha'_{x(v\mp1)} - \frac{2\pi}{m}x\Big)\Big]\Big\} \end{aligned} \tag{12}$$

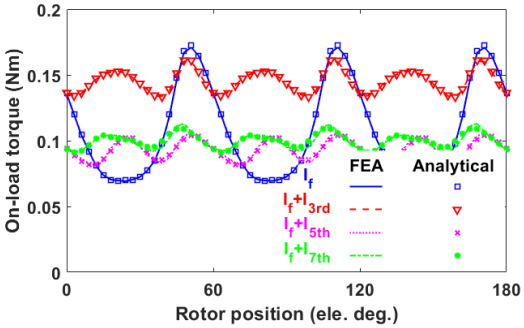

Fig. 4. Comparison of 2D-FE and analytically predicted instantaneous torques for the SL 6-phase DS-SRMs with current harmonic injections. The fundamental current I_f is 1Arms and the characteristics of current harmonic is listed in TABLE II

By way of example, Fig. 4 shows a comparison between 2D-FE and analytical instantaneous torques for the SL 6-phase machine with a range of current harmonic injections. The fundamental current is 1Arms. A generally good agreement can be observed between 2D-FE and analytical predictions at low phase rms current condition. It has been found that the proposed current harmonic injection method is able to mitigate the torque ripple for the m-phase DS-SRMs, if the current harmonic is appropriately selected using the strategy described above.

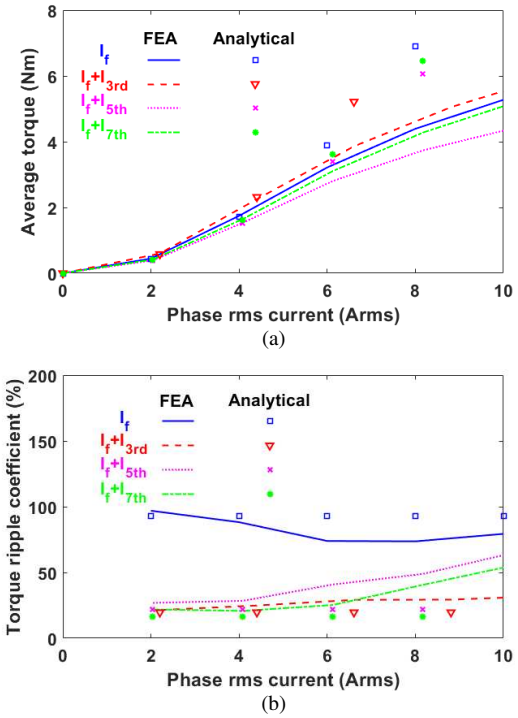

Fig. 5. Comparison of 2D-FE and analytically predicted (a) average torque and (b) torque ripple coefficient *vs* phase rms current for the SL 6-phase DS-SRMs with current harmonic injections. The characteristics of current harmonic are listed in TABLE II.

Fig. 5 shows the average torque and torque ripple coefficient versus phase rms current after current harmonic injection for the SL 6-phase DS-SRM. At a modest phase current (i.e. <4Arms), the proposed model can accurately predict the average torque and torque ripple. However, with increasing phase current, the machine becomes magnetically saturated and there is an increasing discrepancy between the non-linear 2D-FE and the necessarily linear analytical predictions. This illustrates a key limitation of the analytical torque models. However, although the accuracy of the torque equation is diminished at high phase current, the benefits of current harmonic injection on torque ripple reduction is not seriously compromised.

TABLE II. CHARACTERISTICS OF CURRENT HARMONICS TO MINIMIZE TORQUE RIPPLE (Phase RMS current is 1Arms)

Phase Number		3rd		5th		7th	
		mag	phase	mag	phase	mag	phase
4	DL	48.4%	270.8°	64.9%	2.15°	67.2%	87°
	SL	50%	266.1°	35.7%	353.5°	35.3%	87.5°
5	DL	33.6%	71.3°	686%	196.9°	8.66%	90.9°
	SL	32.3%	78.6°	65%	177.7°	8.28%	89.1°
6	DL	1204%	0.06°	34%	113.4°	34.7%	202°
	SL	47.7%	45.1°	21.7%	134.3°	21.7%	223.8°

Once the accuracy of the analytical torque models has been validated by 2D-FEA, at least under non-saturated conditions, it can be utilized to select the current harmonic order to suppress the torque ripple. The methodology is based around generating an opposite torque ripple by the current harmonic to compensate for that produced by fundamental current. A similar method was reported for a 3-phase machine in [12] in order to select the current harmonic required. This has been extended in this paper to minimize the torque ripple of a general m-phase machine, which has been detailed in Appendix. Typical results generated using this method for a series of 4, 5 and 6 phase machines are listed in TABLE II.

The injection of current harmonics will affect the RMS value of the phase current, which may necessitate some modification of the fundamental magnitude to maintain the same RMS. As an example, maintaining the phase RMS current at 1A with the addition of the calculated harmonics leads to the predicted average torque and torque ripple variations shown in TABLE III.

TABLE III. AVERAGE TORQUE AND TORQUE RIPPLE COEFFICIENT AFTER CURRENT HARMONIC INJECTION WITH 1ARMS PHASE CURRENT

Phase Number		3rd		5th		7th	
		Ave (%)	Rip (%)	Ave (%)	Rip (%)	Ave (%)	Rip (%)
4	DL	-94.2	+234.3	-50.4	+85.4	-52.3	+116.2
	SL	-99.7	+2045	+4.1	+12.2	+3.47	+2.0
5	DL	+43.7	-74.7	-98.2	-55.4	+3.0	-81.8
	SL	+45.9	-84.4	-38.7	-68.0	+3.1	-82.2
6	DL	-99.4	-69.5	-46.8	-50.2	-18.4	-49.7
	SL	+10.2	-78.0	-17.2	-72.2	-11.3	-77.8

Note: "+" means increased and "-" means reduced.

It is found that the 3rd order current harmonic shows the best performance for most machines, such as DL/SL 5-phase machines, SL 6-phase machines. It not only reduces the torque ripple by more than 70%, but also increases the average torque for a given RMS level of current, especially, for the 5-phase machines. However, it is ineffective in reducing the torque ripple or increasing the average torque for the DL 6-phase machine even when a 3rd order harmonic as high as 1204% of the fundamental current is injected. This is mainly due to the fact that the harmonic torques due to self- and mutual-inductances have cancelled each other. Similarly, the 5th order current harmonic will not be effective for the DL 5-phase machine. It is also found that, due to the special characteristics of the 4-phase machines, no harmonic current injection can be used for reducing their torque ripple regardless of whether a SL or DL winding structure is adopted. However, the proposed methods can still be used to increase the average torque.

In order to establish the reason why the 4-phase machines do not respond well to harmonic injection, it is useful to consider the torque waveforms of a SL 4-phase DS-SRM with the injected current harmonic characterized in TABLE II which are shown in Fig. 6. It can be seen that after the 3rd order current harmonic is injected, the dominant 4th order torque ripple has been entirely suppressed, as expected. However, although this current harmonic injection has little effect on other harmonics such as the 8th and 12th order torque harmonics, the average torque is very markedly reduced by 99.7%, i.e. close to zero average torque. This is predominantly a consequence of the fact that the 2nd order inductance harmonic (highest magnitude) is an active inductance harmonic ($v \pm 1$) interacting with the 3rd order current harmonic, which significantly reduces the average torque at the selected phase angle. It leads to an extremely high resultant torque ripple coefficient. The 5th and 7th order current harmonics can also suppress the 4th order torque harmonic, in contrast to the 3rd order current harmonic, the 8th order torque harmonic is significantly increased [see Fig. 6 (b)], due to the interaction between current harmonics and the 2nd order

inductance harmonic ($|1 \pm v \pm n|$). Therefore, together with the reduction in the average torque, no obvious improvement is observed in the resultant torque ripple. This is similar for the double layer 4-phase DS-SRM, and therefore the corresponding results have not been shown here to avoid repetition. It is worth noting that due to the nature of inductances of the 4-phase DS-SRMs, their instantaneous torques at some rotor positions, such as 0°, 90° and 180°, etc., are almost zero and cannot be improved by the proposed methods as shown in Fig. 6 (a). Therefore, other methods such as the rotor pole shaping proposed in [7] would be required to modify the inductance profile so as to reduce the torque ripple.

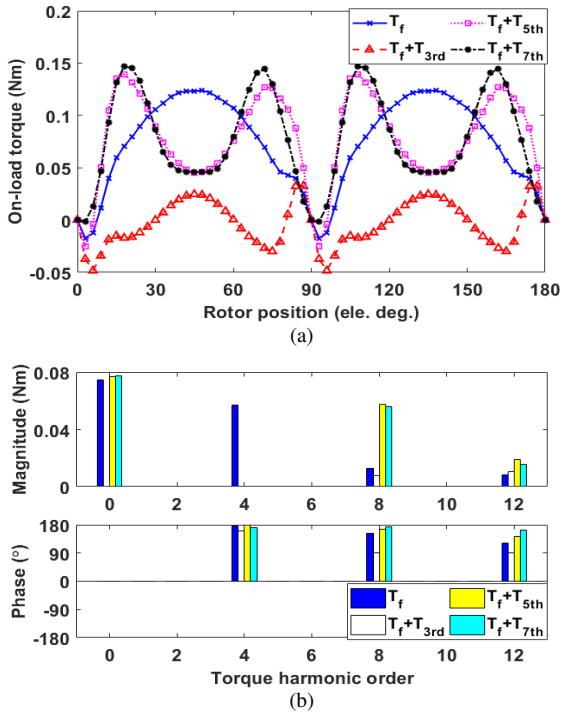

Fig. 6. (a) on-load torque and (b) spectra for single layer 4-phase DS-SRM with predicted current harmonics injected. Phase RMS current is 1A.

III. Losses And Dynamic Performance

Although harmonic current injection can reduce torque ripple and can even increase the average torque for some cases, the high order current harmonic will lead to the extra losses due to the higher frequency. This could diminish the dynamic performance, particularly the efficiency maps of the DS-SRMs. In order to fully investigate the effectiveness of the proposed method for m-phase machines, this section uses a SL 6-phase DS-SRMs as an example to investigate the losses and dynamic performance associated with current harmonic injection. It is worth noting in all cases, the RMS value of the current (I_{RMS}) both with and without current harmonic injection is always maintained at the same value. Moreover, since the machines under consideration are small (i.e. stator diameters of only 45mm) thin gauge copper wires have been utilized, e.g. 0.56mm wire diameter in the case of the SL 6-phase DS-SRM. As a result, when the machines operate at rated speed, the skin effect due to injected high frequency current can be neglected.

A. Iron Losses

In order to calculate the iron losses in the machines, the flux densities in each mesh element (in the 2D FE models) are analyzed using fast Fourier transform, and the iron losses due to each flux density harmonic can be predicted by using (13) [20].

$$P_{Fe} = k_h(f, B_m) f B_m^2 + k_e(f, B_m) f^2 B_m^2 \quad (13)$$

where f is the frequency of stator or rotor flux-density, B_m is the magnitude of alternating flux-density and k_h and k_e are the hysteresis and eddy current loss coefficients, respectively, which are frequency dependent as investigated in [21]. The comparison of iron loss versus phase rms current has been investigated and the results are shown in Fig. 7.

Generally, with the injection of high order current harmonics, it would be expected that the iron loss of the machine would tend to increase. However, it is interesting to note that at currents of<18A or so, the iron loss with the 3rd order current harmonic injection is larger than that with the 5th order current harmonic injection.

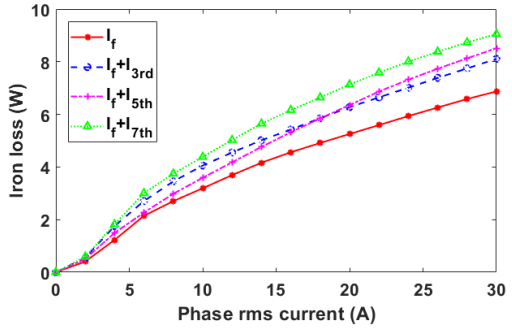

Fig. 7 Comparison of iron loss for SL 6-phase DS-SRM with current harmonic injection. Rotation speed is 400rpm.

In order to investigate this behaviour, it is useful to consider the contribution from the eddy current and hysteresis components of the stator iron loss. These components are summarised at a phase current of 5Arms in Fig. 8. A similar trend has been observed for the rotor losses. It has been found that when the machine is operating at this relatively low current level, both eddy current and hysteresis losses due to fundamental flux density are slightly reduced. This is mainly due to fact that the magnitude of fundamental current is reduced with current harmonic injection in order to maintain the same RMS current. However, the k^{th} order current harmonic injection will increase the losses due to the k^{th} order flux density harmonic. In this case, since larger 3rd order current harmonic is injected, its resultant iron loss could be higher than that with the 5th order current harmonic injection. It is also found in the Fig. 7 that, at higher current level, the iron losses with the 3rd order harmonic current injection can be lower than that of the 5th order harmonic current injection. This is largely due to the different influence of magnetic saturation on the different injected current harmonics.

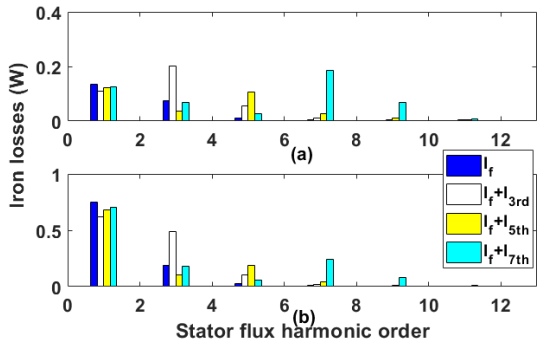

Fig. 8 (a) Eddy current losses and (b) Hysteresis losses for the SL 6-phase DS-SRM. Phase current is 5Arms and rot speed is 400rpm.

B. Torque-Speed Characteristics

Due to the doubly salient structures, the variation in the inductances will inevitably lead to large harmonics in the induced back-EMF, especially when high order current harmonics are injected. This will cause terminal voltage distortion as noted in [22]. This will in turn affect the SVPWM modulation and reduce the voltage utilization ratio. As a result, the base speed of the investigated machines after current harmonic injections will tend to be reduced. To investigate the dynamic performance of the proposed method, the torque-speed characteristics of the investigated DS-SRMs with current harmonic injection have also been studied in this section.

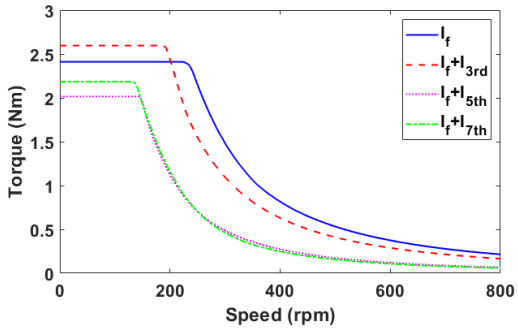

Fig. 9 Torque-speed curve of the SL 6-phase DS-SRM when $I_{max} = 7.07A$ and $V_{dc} = 24$V.

Fig. 9 shows the predicted torque-speed curve for the SL 6-phase DS-SRM when the current limit is 7.07A (5Arms) and the dc-link voltage is 24V. It shows that the 3rd order current harmonic can increase the average torque in the constant torque region and slightly reduce the torque capability compared with the fundamental current supply in the flux weakening region. It is not surprising that the 5th and 7th order current harmonics will reduce the performance in both constant torque and flux weakening regions. This is due to the fact that they reduce the output torque and increase the voltage distortion, leading to limited flux weakening capability.

C. Efficiency Maps

Due to a relatively low rotor speed, the mechanical losses have been neglected and the efficiency can be reasonably approximated as:

$$\eta = \frac{P_{out}}{P_{out} + P_{copper} + P_{Fe}} \tag{14}$$

where P_{out} is the output power and can be calculated from $\omega_m T_e$.

The efficiency maps with and without current harmonic injection have been calculated, as shown in Fig. 10. It can be seen that a maximum efficiency of 72% is achieved by the 3rd order current harmonic injection between 1000rpm and 1500rpm. Although the efficiency at base speed with the 3rd order current harmonic injection is reduced, it can still increase the efficiency in the lower speed region, due to extra torque production. However, the 5th and 7th order current harmonic injections degrade the efficiency across the full speed range. A modest efficiency of 64% can be achieved at speeds ~600 rpm.

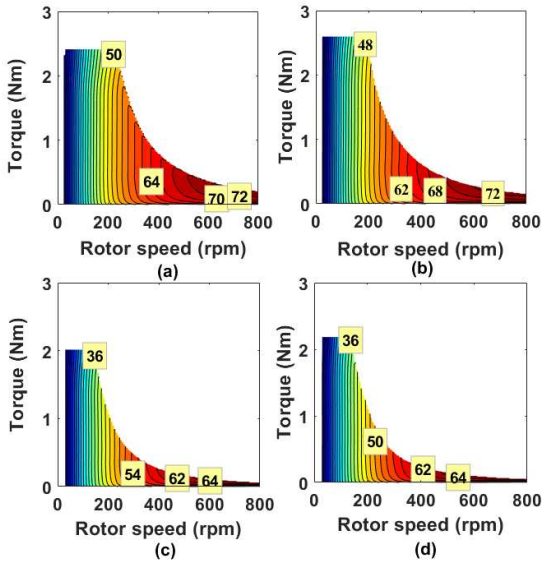

Fig. 10 Efficiency maps of the SL 6-phase DS-SRM with/without current harmonic injections. $I_{max} = 7.07A$ and $V_{dc} = 24$V. (a) fundamental, (b) 3rd order, (c) 5th order and (d) 7th order.

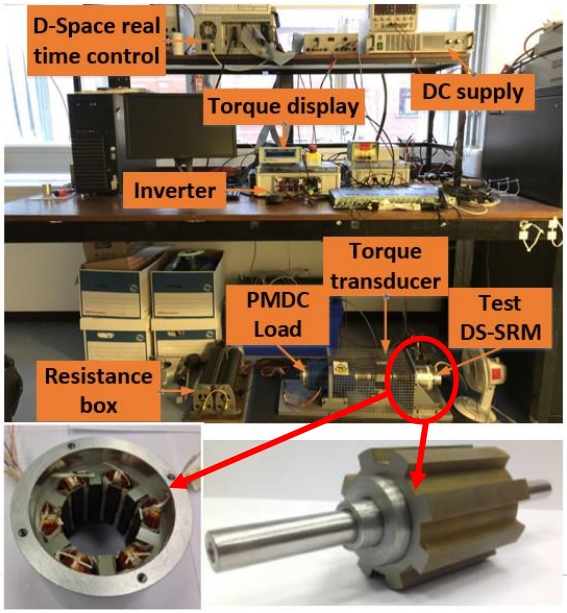

Fig. 11. Test rig and prototype machine for dynamic tests.

IV. Experimental Validation

In order to validate the effectiveness of the proposed current harmonic injection method and also the predictions in previous sections, a SL 6-phase DS-SRM (12s/8p) was experimentally tested. It is worth mentioning that this machine is converted from an existing SL 3-phase DS-SRM which was initially

designed in [5]. As a result, the number of turns per phase was reduced by half (66) rather than 132 used in previous sections. This means that the inductance will be reduced by a factor of four, which leads to a four-fold reduction in the average torque in the experimental validation section compared with the simulated torque in Sections II and III. However, this will not influence the effectiveness of the proposed method as it can be used in any synchronous reluctance machines. Fig. 11 shows the test rig setup for validating the proposed harmonic current injection method.

The 6-phase machine is controlled as a dual 3-phase machine (phases A, C and E form one set, while phases B, D and F form the second set) with a phase shift of 60 electrical degree between the two sets, as shown in Fig. 12. Two 3-phase winding sets are supplied by two 3-phase half bridge voltage source inverters (VSIs), which are controlled using conventional space vector pulse width modulation (SV-PWM). The harmonic injection block is detailed in [12]. It is worth noting that in order to inject a 3rd order current harmonic into a 6-phase machine, two extra half-bridges are required to control the zero-sequence current. However, due to the hardware limitations, only the 5th and 7th order harmonic injections have been carried out in this section.

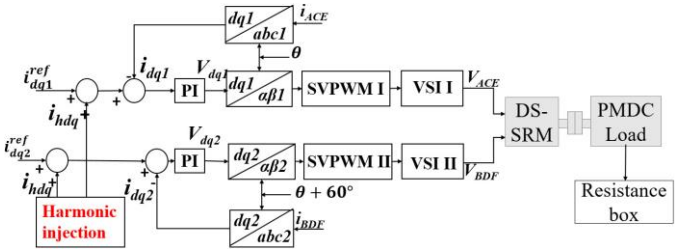

Fig. 12. Current control block diagram of the 6-phase prototype machine.

A. Steady-State Tests

The first test evaluated the performance of the proposed current harmonic injection method in steady-state. Therefore, the machine is operating under current control with a reference current level of 5Arms. A permanent magnet (PM) direct current (DC) machine was used to provide a load for the SL 6-phase DS-SRM machine under test. Fig. 13 shows the current, speed and torque waveforms. As will be evident, with 5th and 7th order current harmonic injection (Listed in TABLE II), the speed and torque ripple can be markedly reduced, but at the expense of a 14% reduction in average torque. Moreover, due to the fact that the PM DC machine provides a passive load for the prototype machine, the average load torque is simply proportional to the rotor speed and can be measured by torque transducer. The average load torques are around 0.67Nm, 0.56Nm and 0.58Nm for the fundamental, 5th and 7th order current harmonic injection, respectively.

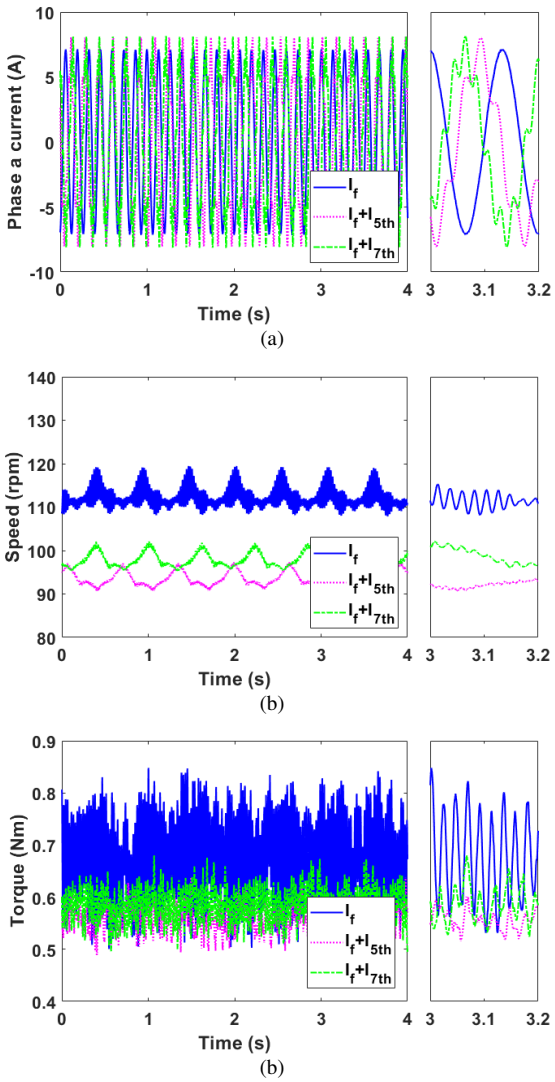

Fig. 13 (a) phase a currents, (b) speeds and (c) torques. Phase RMS current is 5A.

Fig. 14 shows the torque spectra during one electric period. It is apparent that the 6th order torque harmonic can be suppressed by 85% and 70%, respectively, with the 5th and 7th order current harmonic injections, which generally agree with the predictions observed in TABLE III. It is worth noting that the active inductances which produce a contribution to the average torque for the 5th order current harmonic are 4th and 6th (5 ± 1), while those for the 7th order current harmonic are 6th and 8th (7 ± 1). And the magnitude of the 4th order inductance harmonic is much larger than the 8th order inductance harmonic. As a result, the 5th order current harmonic is much more sensitive to average torque than the 7th order current harmonic. Therefore, to reduce the torque ripple by the same degree, the reduction in average torque for the 5th order current harmonic injection is more obvious. Moreover, the low frequency harmonics in the torque waveform are due to unavoidable mechanical imbalance of the test rig and also the inherent torque ripple of the PMDC load machine.

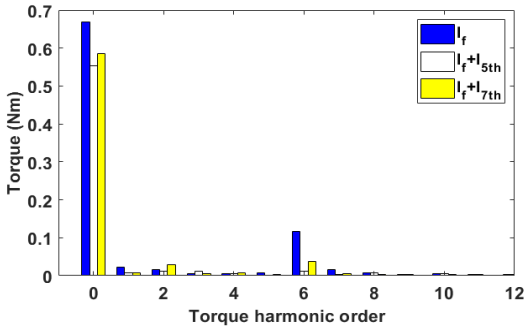

Fig. 14. Spectra of torque at 5A phase RMS current with and without current harmonic injections.

B. Transient-State Tests

The second test investigated the effectiveness of the current harmonic injection method in a transient mode of operation with the machine operating under speed control. The initial speed was set to 100rpm and after 3s, the speed reference increases to 400rpm. Again, both the 5th and 7th order current harmonics were injected and the current limit of speed controller is 5Arms. Fig. 15 shows the *d*- and *q*-axis current references and feedbacks of the current regulators and Fig. 16 shows the difference between the feedback and the reference currents. It can be found that increasing rotor speed and load torque will indeed affect the current regulator performance. A slight phase delay will occur when machine operates at rated speed, leading to ±0.5A current error (±6%).

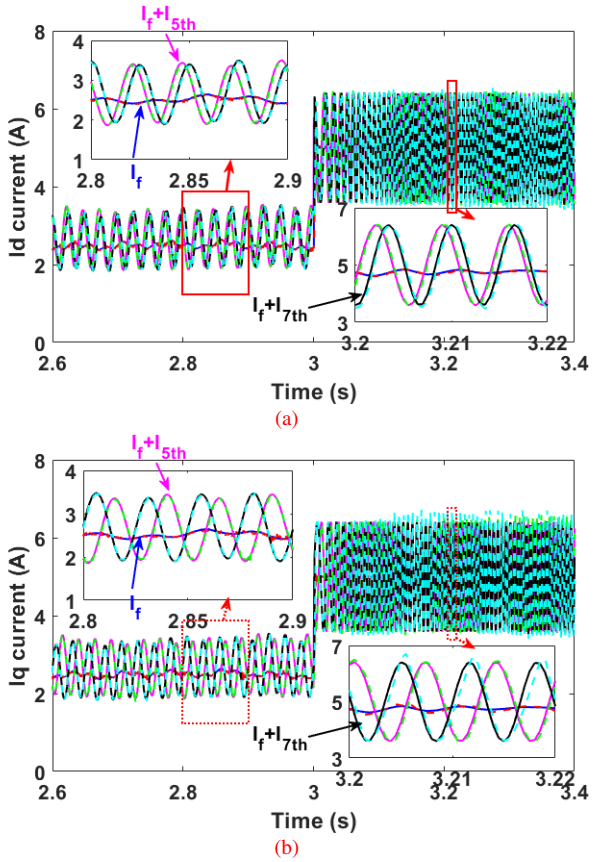

(a)

(b)

Fig. 15 Transient-state results (a) i_d and (b) i_q. (solid line: reference; dashed line: feedback).

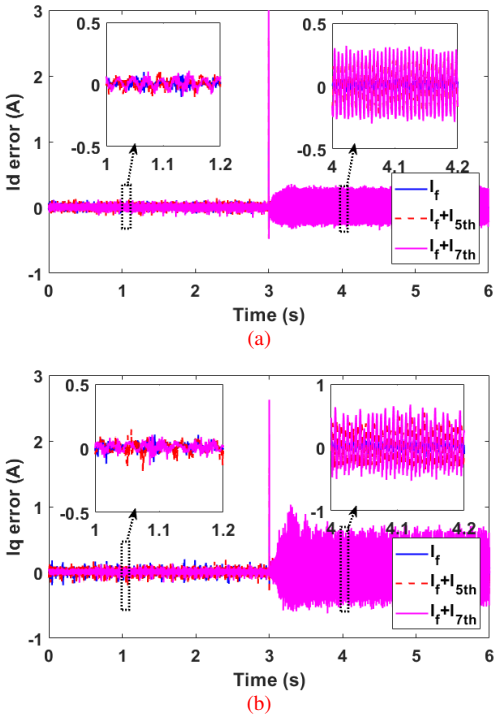

(a)

(b)

Fig. 16 Transient-state results (a) i_d error and (b) i_q error.

The speed and torque responses for different harmonics are shown in Fig. 17 (a) and (b), respectively. It can be seen that the speed and torque ripple suppression of the proposed method is not compromised during transient operation. However, the time taken to accelerate from 100rpm to 400rpm increases by ~17% and 15% with 5th and 7th order current harmonic injection respectively, in large part as a consequence of the reduction in the average torque resulting from harmonic current injection.

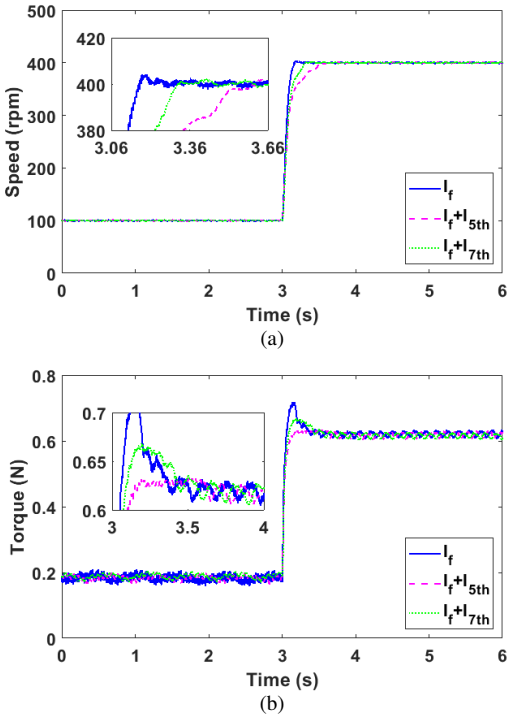

(a)

(b)

Fig. 17 Transient-state results. The speed steps up from 50rpm to 200rpm. (a) Speed and (b) Torque.

C. Torque- and Efficiency-Speed Curves

In addition to the steady and transient-state tests, the torque- and efficiency-speed curves were also derived from experimental measusrements. The current and dc voltage limits were set to the same values as section III.B, i.e. 7.07A (5Arms) and 24V, respectively. Fig. 18 shows the torque- and efficiency-speed characterisitc for the test machine. It is worth noting that the significant reduction in the average torque level compared with preditions in Fig. 9 is due to reduced number of turns per phase of the protype machineas explained at the beginning of the section IV. For the same reason, the induced voltage is reduced by half that predicted. When due account is taken of the scaling for the reduced number of turns, the measured results match well with predictions. As anticipated in both in the contant-torque and flux-weakening regions of operation, the 5th and 7th order current harmonic injections cannot produce the same average torque as that produced with a fundmental current.The base-speed of the torque-speed characterisitc is reduced, due to significant voltage distortion caused by the interation between the current and inductance harmonics. Moreover, the 5th and 7th order current harmonic injections tend to reduce the machine efficiency in full speed range. It is worth mentioning that small diameter copper wires have been delibrately used to ease the winding process of the prototype machine resulting in a modest coil packing factor. This inevitably increases the phase resistance. As a result, this small prototype machine only achieved modest levels of efficiency.

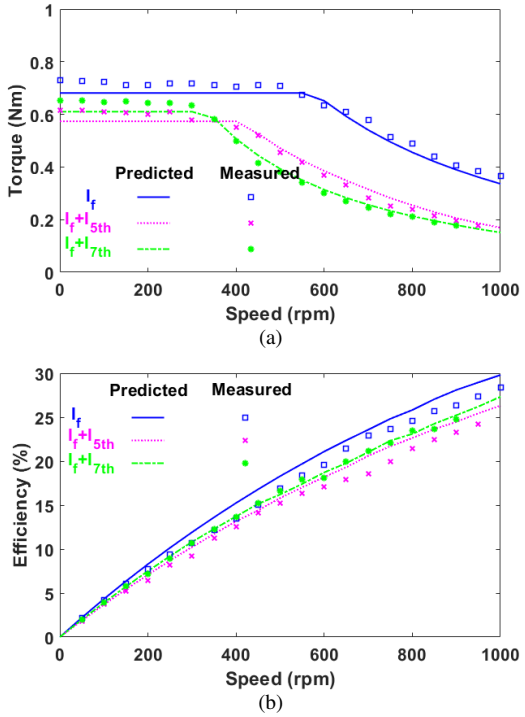

Fig. 18 Predicted and measured torque- and efficiency-speed curves. (I_{max} = 7.07A and V_{dc}=24V) (a) torque-speed curves and (b) efficiency-speed curves.

V. Conclusion

This paper has investigated the influence of harmonic current injection on electromagnetic performance of multi-phase DS-SRMs with different slot/pole combinations, winding configurations and phase numbers. It has found that when the v^{th} order current harmonic is injected in a m-phase machine, there will be two active inductance harmonics [$(v \pm 1)^{th}$] producing extra average torque. Compared with other current harmonics, the 3rd order current harmonic shows the best potential in average torque improvement but has the drawback of requiring reconfiguration of the drive to accommodate zero sequence currents. Moreover, it is also found that the active inductances for torque ripple reduction [$(|mk \pm v \pm 1|)^{th}$] depend on the phase number m and the injected current harmonic order v. If the 2nd order inductance harmonic is one of the active inductance harmonics, lower (in terms of magnitude) current harmonic is required to completely compensate the dominant torque harmonic due to fundamental current.

With appropriate selection of injected harmonic currents, some aspects of performance of the machine such as efficiency at constant torque region can be improved and the same flux weakening capability as pure fundamental current supply can be maintained. The effectiveness of the proposed method is verified by 2D-FEA and the majority of the predictions have been validated by experiments using a single layer 6-phase DS-SRM.

Appendix

The torque production by pure fundamental current for multi-phase DS-SRM has been investigated in [15]. It has been found that the mkth order torque harmonic (T_{frip_mkth}) can be calculated by

$$T_{frip\_mkth} = T_{Frip}\sin(mk\theta_e + \varphi_{Frip}) \tag{15}$$

where T_{Frip} and φ_{Frip} are the resultant magnitude and phase angle of certain order torque ripple, which can be calculated by the analytical model developed in [15]. Based on the analytical model in this paper, it can be demonstrated that current harmonics can also produce the mkth order torque harmonic, which can be used to compensate the torque produced by fundamental current, leading to reduced resultant torque ripple. By way of example, in order to reduce the 6th (mk=6) order torque harmonic in 6-phase machines by injecting the 3rd order current harmonic (v=3), there will be four active inductances that contribute to the 6th order torque harmonic, viz. 2th, 4th, 8th and 10th, respectively. It is worth noting that the self- and mutual-torque terms due to the same active inductance harmonic have the same factor (A, B, C or D). Moreover, the torque terms due to two active inductance harmonics ($|mk - v \pm 1|$) show the same sign between θ_e and β_v, while the other two ($|mk + v \pm 1|$) present different signs. Therefore, the torque ripple performance after current harmonic injection can be simply written as

$$\begin{aligned} T_{hrip}(\beta_v) &= \sum_{i=1}^{(2Z+1)\times 2} T_{Xi}\sin(mk\theta_e + \varphi_{Xi} + \beta_v) \\ &\quad + T_{Yi}\sin(mk\theta_e + \varphi_{Yi} - \beta_v) \\ &= T_{Xrip}\sin(mk\theta_e + \varphi_{Xrip} + \beta_v) \\ &\quad + T_{Yrip}\sin(mk\theta_e + \varphi_{Yrip} - \beta_v) \\ &= T_{Hrip}(\beta_v)\sin\left(mk\theta_e + \varphi_{Hrip}(\beta_v)\right) \end{aligned} \tag{16}$$

with

$$\begin{cases} \tan\left(\varphi_{Hrip}(\beta_v)\right) = \dfrac{B(\beta_v)}{A(\beta_v)} \\ T_{Hrip}(\beta_v) = \sqrt{A^2 + B^2} \end{cases} \tag{17}$$

$$\begin{cases} A = T_{Xrip}\cos\left(\varphi_{Xrip} + \beta_v\right) + T_{Yrip}\cos\left(\varphi_{Yrip} - \beta_v\right) \\ B = T_{Xrip}\sin\left(\varphi_{Xrip} + \beta_v\right) + T_{Yrip}\sin\left(\varphi_{Yrip} - \beta_v\right) \end{cases} \tag{18}$$

where X and Y $[X, Y \in (A, B, C, D)]$ represent the torque terms with the same or different sign between θ_e and β_v, respectively. T_{Xi}, T_{Yi}, φ_{Xi} and φ_{Yi} [i=1, 2 …$(2Z+1)\times 2$] are all constant, representing the magnitude and phase angle for the relative torque terms, when β_v is 0. It can be observed that the resultant torque ripple harmonic can be controlled by β_v. It is worth noting that the resultant magnitude T_{Hrip} is also proportional to the injected current harmonic magnitude i_v. Therefore, in order to minimize the resultant torque ripple, (5) and (16) need to achieve the same magnitude and have a π phase difference, which leads to

$$\begin{cases} \varphi_{Hrip}(\beta_v) = \varphi_{Frip} + \pi \\ T_{Hrip}(I_v, \beta_v) = T_{Frip} \end{cases} \tag{19}$$

By solving (19), the harmonic magnitude and phase angle can be predicted at which the minimum torque ripple will be achieved.

REFERENCES

[1] C. Gan, J. Wu, Q. Sun, W. Kong, H. Li, and Y. Hu, "A review on machine topologies and control techniques for low-noise switched reluctance motors in electric vehicle applications," *IEEE Access,* vol. 6, pp. 31430-31443, May 2018.

[2] G. J. Li, X. Ojeda, S. Hlioui, E. Hoang, M. Gabsi, and C. Balpe, "Comparative study of Switched Reluctance Motors performances for two current distributions and excitation modes," in *IECON '09. 35th Annual Conference of IEEE Industrial Electronics*, 2009.

[3] X. Liu, Z. Q. Zhu, M. Hasegawa, A. Pride, and R. Deodhar, "Investigation of PWMs on vibration and noise in SRM with sinusoidal bipolar excitation," presented at the in Proc. 21th IEEE International Symposium on Ind. Electron., Hangzhou, China, pp. 674-679, 2012.

[4] C. M. Donaghy-Spargo, B. C. Mecrow, and J. D. Widmer, "On the influence of increased stator leakage inductance in single-tooth wound synchronous reluctance motors," *IEEE Trans. Ind. Electron.,* vol. 65, no. 6, pp. 4475-4482, Jun. 2018.

[5] X. Y. Ma, G. J. Li, G. W. Jewell, Z. Q. Zhu, and H. L. Zhan, "Performance comparison of doubly salient reluctance machine topologies supplied by sinewave currents," *IEEE Trans. Ind. Electron.,* vol. 63, no. 7, pp. 4086 - 4096, Jul. 2016.

[6] X. Y. Ma, G. J. Li, Z. Q. Zhu, G. W. Jewell, and J. Green, "Investigation on synchronous reluctance machines with different rotor topologies and winding configurations," *IET Elect. Power Appl.,* vol. 12, no. 1, pp. 45-53, Jan. 2018.

[7] G. Li, J. Ojeda, S. Hlioui, E. Hoang, M. Lecrivain, and M. Gabsi, "Modification in rotor pole geometry of mutually coupled switched reluctance machine for torque ripple mitigating," *IEEE Trans. Magn.,* vol. 48, no. 6, pp. 2025-2034, Jun. 2012.

[8] H. Y. Yang, Y. C. Lim, and H. C. Kim, "Acoustic noise/vibration reduction of a single-phase SRM using skewed stator and rotor," *IEEE Trans. Ind. Electron.,* vol. 60, no. 10, pp. 4292-4300, Oct. 2013.

[9] R. B. Inderka and R. A. A. D. Doncker, "DITC—Direct instantaneous torque control of switched reluctance drives," *IEEE Trans. Ind. Appl.,* vol. 39, no. 4, pp. 1046 - 1051, Jul.-Aug. 2003.

[10] C. Lai, G. Feng, K. Mukherjee, V. Loukanov, and N. C. Kar, "Torque ripple modeling and minimization for interior PMSM considering magnetic saturation," *IEEE Trans. Power Electron.,* vol. 33, no. 3, pp. 2417-2429, Mar. 2018.

[11] F. Erken, E. Öksüztepe, and H. Kürüm, "Online adaptive decision fusion based torque ripple reduction in permanent magnet synchronous motor," *IET Ele. Power Appl.,* vol. 10, no. 3, pp. 189-196, Mar. 2016.

[12] G. Li, K. Zhang, Z. Q. Zhu, and G. Jewell, "Comparative studies of torque performance improvement for different doubly salient synchronous reluctance machines by current harmonic injection," *IEEE Trans. Energy Conver.,* pp. 1-1, Sep. 2018.

[13] K. Zhang, G. J. Li, Z. Q. Zhu, and G. W. Jewell, "Torque performance improvement of doubly salient synchronous reluctance machines by current harmonic injection," *in Proc. IEEE Int. Ele. Mach. & Dri Conf (IEMDC),* pp. 1222-1227, 12-15 May 2019.

[14] J. Baek, S. S. R. Bonthu, and S. Choi, "Design of five-phase permanent magnet assisted synchronous reluctance motor for low output torque ripple applications," *IET Ele. Power Appl.,* vol. 10, no. 5, pp. 339-346, 2016.

[15] K. Zhang, G. J. Li, Z. Q. Zhu, and G. W. Jewell, "Investigation on contribution of inductance harmonics to torque production in multiphase doubly salient synchronous reluctance machines," *IEEE Trans. Mag.,* vol. 55, no. 4, pp. 1-10, Apr. 2019.

[16] A. Arafat, S. Choi, and J. Baek, "Open-phase fault detection of a five-phase permanent magnet assisted synchronous reluctance motor based on symmetrical components theory," *IEEE Trans. Ind. Electron.,* vol. 64, no. 8, pp. 6465-6474, Aug. 2017.

[17] L. A. Pereira, S. Haffner, G. Nicol, and T. F. Dias, "Multiobjective optimization of five-phase induction machines based on NSGA-II," *IEEE Trans. Ind. Electron.,* vol. 64, no. 12, pp. 9844-9853, Dec. 2017.

[18] K. Wang, Z. Y. Gu, C. Liu, and Z. Q. Zhu, "Design and analysis of a five-phase spm machine considering third harmonic current injection," *IEEE Trans. Energy Conver.,* vol. 33, no. 3, pp. 1108-1117, Sep. 2018.

[19] Y. Hu, Z. Q. Zhu, and M. Odavic, "Torque capability enhancement of dual three-phase pmsm drive with fifth and seventh current harmonics injection," *IEEE Trans. Ind. Appl.,* vol. 53, no. 5, pp. 4526-4535, Sep. 2017.

[20] H. Domeki, Y. Ishihara, C. Kaido, Y. Kawase, S. Kitamura, T. Shimomura*, et al.*, "Investigation of benchmark model for estimating iron loss in rotating machine," *IEEE Trans. Mag.,* vol. 40, no. 2, pp. 794-797, 2004.

[21] K. Zhang, G. J. Li, R. Zhou, Z. Q. Zhu, and G. W. Jewell, "Losses in different doubly salient synchronous reluctance machines with current harmonic injection," *Int. Conf. Ele. Mach. Sys. (ICEMS),* pp. 1-6, 11-14 Aug. 2019.

[22] D. Wu, Z. Q. Zhu, and W. Chu, "Reduction of on-load terminal voltage distortion in fractional slot interior permanent magnet machines," *IEEE Trans. Energy Convers.,* vol. 31, no. 3, pp. 1161-1169, Sep. 2016.